

Planetary Defense Mission Design Using an Asteroid Mission Design Software Tool (AMiDST)

George Vardaxis* and Bong Wie†

Iowa State University, Ames, Iowa 50011, USA

Tracking the orbit of asteroids and planning for asteroid missions have ceased to be a simple exercise, and become more of a necessity, as the number of identified potentially hazardous near-Earth asteroids increases. Several software tools such as Mystic, MALTO, Copernicus, SNAP, OTIS, and GMAT have been developed by NASA for spacecraft trajectory optimization and mission design. However, this paper further expands upon the development and validation of an Asteroid Mission Design Software Tool (AMiDST), through the use of approach and post-encounter orbital variations and analytic keyhole theory. Combining these new capabilities with that of a high-precision orbit propagator, this paper describes fictional mission design examples of using AMiDST as applied to comet 2013 A1 and a fictitious asteroid 2013 PDC-E. During the 2013 Planetary Defense Conference, the asteroid 2013 PDC-E was used for an exercise where participants simulated the decision-making process for developing deflection and civil defense responses to a hypothetical asteroid threat.

I. Introduction

Traditional trajectory and mission optimization tools (such as Mystic, MALTO, Copernicus, SNAP, OTIS, and GMAT) are high-fidelity computer programs being developed by NASA [1, 2]. A commonality of all these tools is that they primarily look at the intermediate stage of a mission, the mission trajectory from the current location to desired target - more or less overlooking the other two stages of any mission design, in comparison. An on-line mission design tool to aid in the design and understanding of kinetic impactors necessary for guarding against objects on an Earth-impacting trajectory is being developed at The Aerospace Corporation [3]. Still under development, this on-line tool has hopes of incorporating several specific design variables and limitations to allow for only feasible mission designs based on current launch and mission capabilities.

The Asteroid Mission Design Software Tool (AMiDST) being developed at the Asteroid Deflection Research Center (ADRC) at Iowa State University [4–6] does not yet have the high fidelity as many existing optimization-based packages. However, the focus of the program lies on the launch and terminal phase of a near-Earth object (NEO) mission rather than finding the optimal mission trajectory. Looking into several launch vehicle and spacecraft configurations to complete a given mission design to a designated target NEO, the AMiDST evaluates the possible combinations based upon several evaluation criteria such as launch vehicle mass capacity, mission ΔV requirements, and excess launch vehicle ΔV . In addition to these features, it also provides the estimated total mission cost, used as a main determining factor between mission configurations. A flowchart illustration of the basic algorithms used by AMiDST is presented in Figure 1. In this figure, HAIV stands for Hypervelocity Asteroid Intercept Vehicle and KI for Kinetic Impactor, and NED for Nuclear Explosive Payload, described in details by Pitz et al. [7, 8].

For a current version of AMiDST, the terminal phase of a NEO mission is limited, at this time, to kinetic impact perturbations applied to the target NEO's orbital trajectory. Taking the output of the mission analysis of relative impact angle and velocities of both the spacecraft and target NEO, along with the mass of both objects, the trajectory of the perturbed asteroid would be tracked in order to find how much the trajectory is altered from the previous unperturbed orbit. In addition to simply tracking the NEO to a future time, a resonance and keyhole analysis would be performed to see the likelihood the body would have a further future threat to the Earth.

*Graduate Student, Asteroid Deflection Research Center, Department of Aerospace Engineering, 1200 Howe Hall.

†Vance Coffman Endowed Chair Professor, Asteroid Deflection Research Center, Department of Aerospace Engineering, 1200 Howe Hall.

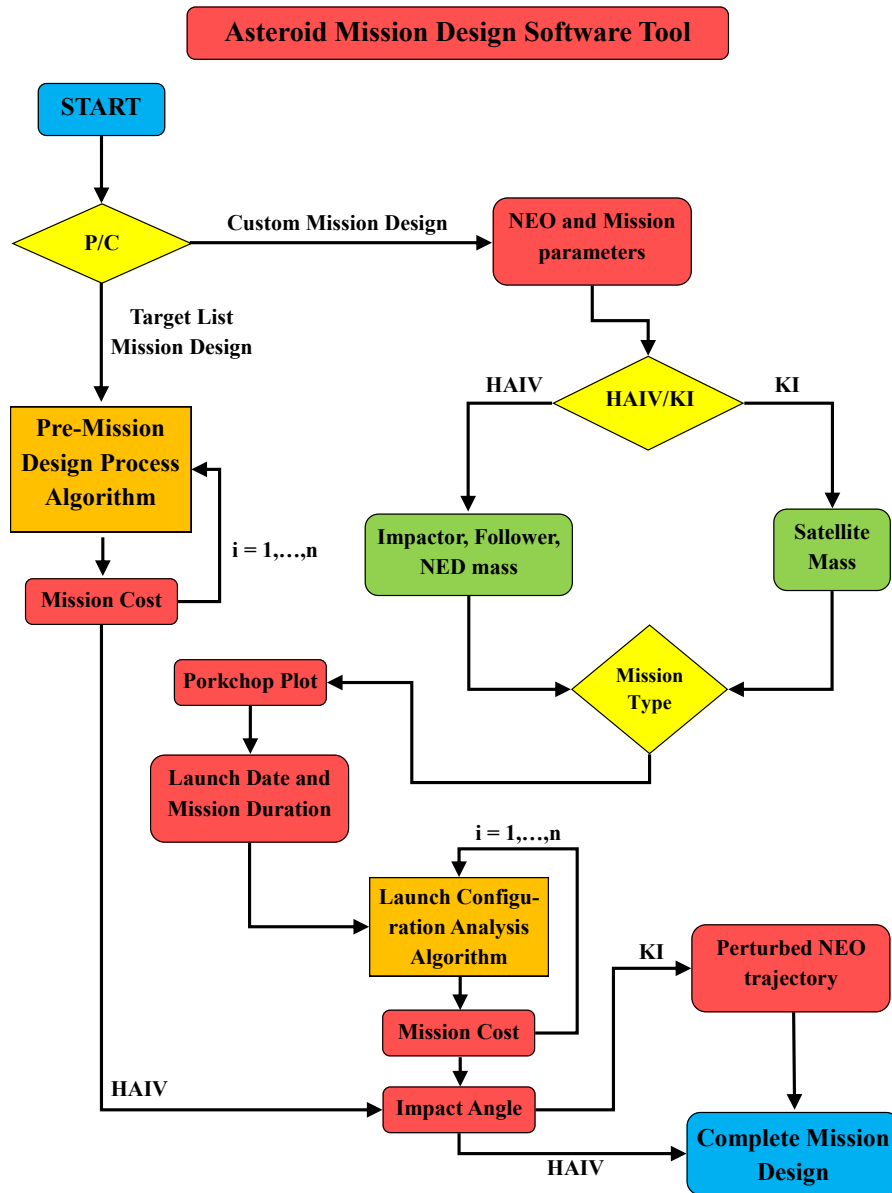


Figure 1. Flowchart illustration of the AMiDST.

II. Mission Design for Asteroids with No Keyholes

Near-Earth objects (NEOs) are asteroids and comets with perihelion distance (q) less than 1.3 astronomical units (AU). The vast majority of NEOs are asteroids, which are referred to as near-Earth asteroids (NEAs). NEAs are divided into three groups (Aten, Apollo, Amor) based on their perihelion distance, aphelion distance (Q), and semi-major axes (a). Of these three classes of asteroids, Aten and Apollo type asteroids are of particular interest to this study due to their relative proximity and Earth impacting potential. Atens are Earth-crossing NEAs with semi-major axes smaller than Earth's ($a < 1.0$ AU, $Q > 0.983$ AU). Apollos are Earth-crossing NEAs with semi-major axes larger than Earth's ($a > 1.0$ AU, $q < 1.017$ AU) [9]. Figure 2 shows representative orbits for the three class of asteroids in reference to Earth's orbit. With the wide array of choices to select target NEOs from, there have been many objects studied through the use of AMiDST [4–6]. The most notable targets being Apophis, 1999 RQ36, 2011 AG5, 2012 DA14, and comet 2013 A1.

In 1990, Congress directed NASA to increase the rate of discovery of near Earth objects [10]. Through those

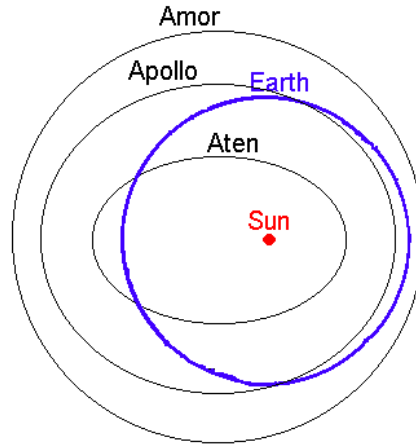


Figure 2. Typical orbits of Apollo, Aten, and Apollo asteroids.

efforts, at times objects of significant size have been found to be on a potential Earth-impacting trajectory. The accurate prediction of such Earth-impacting trajectories could be obtained through the use of high-fidelity N-body models, also containing the effects of non-gravitational orbital perturbations such as solar radiation pressure (SRP). From such highly precise asteroid orbits, many advantages can be had: more specific mission planning, higher certainty of the target's location, and more accurate impact probability.

II.A. Orbit Simulation

The orbital motion of an asteroid is governed by a so-called Standard Dynamical Model (SDM) of the form

$$\frac{d^2\vec{r}}{dt^2} = -\frac{\mu}{r^3}\vec{r} + \sum_{k=1}^n \mu_k \left(\frac{\vec{r}_k - \vec{r}}{|\vec{r}_k - \vec{r}|^3} - \frac{\vec{r}_k}{r_k^3} \right) + \vec{f} \quad (1)$$

where $\mu = GM$ is the gravitational parameter of the Sun, n is the number of perturbing bodies, μ_k and \vec{r}_k are the gravitational parameter and heliocentric position vector of perturbing body k , respectively, and \vec{f} represents other non-conservative orbital perturbation acceleration. The gravitational model used in orbit propagation takes into account the effects of the Sun, all eight planets, Pluto, Ceres, Pallas, and Vesta.

Previous studies performed at the ADRC were concerned with the impact probability of potential Earth-impacting asteroids, such as Apophis, 1999 RQ36, and 2011 AG5 due to their proximity to Earth and their relatively high impact probability. Using commercial software such as NASA's General Mission Analysis Tool (GMAT), AGI's Satellite Tool Kit (STK), and Jim Baer's Comet/asteroid Orbit Determination and Ephemeris Software (CODES), the ADRC conducted precision orbital simulation studies to compare with JPL's Sentry program [11].

II.B. Previous Work

Taking Apophis as a reference NEO, simulations have been run from an initial epoch of August 27, 2011 until January 1, 2037 to show the capabilities of the ADRC's N-body code in calculating precise, long-term orbit trajectories. A preliminary test was conducted for the period of May 23, 2029 to May 13, 2036 show the relative errors of GMAT and STK to JPL's Sentry (Horizons), as well as the error of the N-body code with respect to Sentry. The error in the radial position of Apophis between the N-body code to that of JPL's Sentry is much lower than that of both GMAT and STK. The N-body simulator used to obtain the aforementioned results uses a Runge-Kutta Fehlberg (RKF) 7(8) fixed-timestep method, including the orbital perturbations of all eight planets, Pluto, and Earth's Moon, in the form of constant orbital element rates coupled with the nominal element values provided updated position and velocity data for the perturbation bodies [4].

II.C. Current Work and Capabilities

The fixed timestep numerical integration algorithm has been changed to a variable step method, expanding upon the work done on the numerical integration scheme used to obtain the results previously discussed. The Runge-Kutta Fehlberg method is used for approximating the solution of a differential equation $\dot{x}(t) = f(x, t)$ with initial condition $x(t_0) = c$. The implementation evaluates $f(x, t)$ thirteen times per step using embedded seventh order and eighth order Runge-Kutta estimates to estimate not only the solution but also the error. By specifying the interval in which the results of the integration should be reported and the acceptable local error tolerance, the algorithm takes as many error controlled steps as necessary to calculate the state vector at the desired time.

Orbital data from all chosen planetary bodies is taken for a given period of time to construct a planetary state vector (X, Y, Z, V_X, V_Y, V_Z) database using ephemeris data from the NASA Jet Propulsion Laboratory (JPL) Horizons website. An interpolation scheme is constructed in order to accommodate the need to retrieve data at any specified date within the propagation time period. Using the Julian Date of the available state vector data for each planet as the distinct independent variables of an n -th degree interpolating polynomial, a unique polynomial $P(x)$ is created for each state, which is then applied to each body.

The three most well-known non-conservative perturbations are solar radiation pressure, relativistic effects, and the Yarkovsky effect - the former two being the most prevalent being the former two effects. Solar radiation pressure provides an radial outward force on the asteroid body from the interaction of the Sun's photons impacting the asteroid surface. An SRP model is given by

$$\vec{a}_{SRP} = (K)(C) \left(\frac{A}{M} \right) \left(\frac{L}{4\pi cr^3} \right) \vec{r} \quad (2)$$

where \vec{a}_{SRP} is the acceleration vector due to the solar radiation pressure, C is the coefficient for solar radiation, A is the cross-sectional area presented to the Sun, M is the mass of the asteroid, K is the fraction of the solar disk visible at the asteroid's location, L is the luminosity of the Sun, c is the speed of light, and \vec{r} and r is the distance vector and magnitude of the asteroid from the Sun, respectively.

The relativistic effects of the body are included because for many objects, especially those with small semi-major axes and large eccentricities, those effects introduce a non-negligible radial acceleration toward the Sun. One form of the relativistic effects is represented by

$$\vec{a}_R = \frac{k^2}{c^2 r^3} \left[\frac{4k^2 \vec{r}}{r} - \left(\dot{\vec{r}} \cdot \dot{\vec{r}} \right) \vec{r} + 4 \left(\vec{r} \cdot \dot{\vec{r}} \right) \dot{\vec{r}} \right] \quad (3)$$

where \vec{a}_R is the acceleration vector due to relativistic effects, k is the Gaussian constant, \vec{r} is the position vector of the asteroid, and $\dot{\vec{r}}$ is the velocity vector of the asteroid. With the introduction of such non-conservative forces the error within the system will increase, but these effects need to be included in calculations in order to maintain consistency with the planetary ephemeris. A more complete dynamical model will allow the accurate calculation of asteroid impact probabilities and gravitational keyholes, leading to more effective mission designs [12].

II.D. Fictional Mission Design for Comet 2013 A1 (with No Keyholes)

Comet 2013 A1, an Oort cloud comet, was discovered on January 3, 2013 at the Siding Spring Observatory. The significance of this discovery lies in its anticipated trajectory through our Solar System. On October 19, 2014, comet 2013 A1 is predicted to have a close-encounter with Mars. The nucleus of the comet is estimated to be between one and three kilometers, traveling at 56 km/s. If the comet were to hit Mars, the amount of impact energy would be about a third of the energy from the asteroid that killed off the dinosaurs and about 80 million times more energy than the 17-m asteroid that exploded over Russia this past February. Table 1 shows the orbital elements of comet 2013 A1 [9].

Because comet 2013 A1 is in a heliocentric hyperbolic orbit, there is a limited window in which we could design a feasible mission to this comet. Figure 3 shows its orbital trajectory illustration.

Table 1. (a, e, i) of comet 2013 A1.

Orbital Element	Value	Uncertainty (1- σ)	Units
a	-3842.815	646.13	AU
e	1.000364	6.1198e-05	
i	129.0223	0.002152	deg

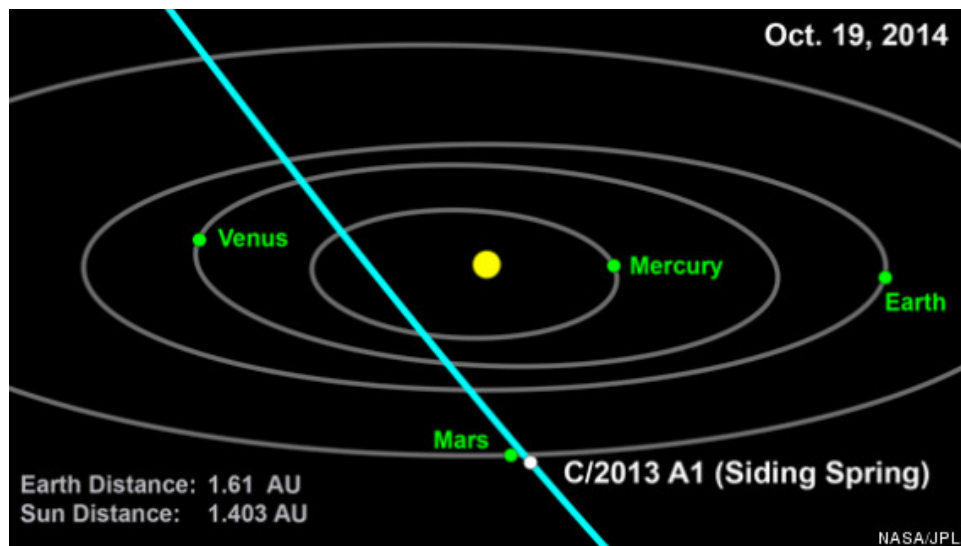


Figure 3. Orbital illustration of comet 2013 A1.

At this point in time we assume that it is currently the beginning of January 2013 and comet 2013 A1 has just been discovered and based on the simulations it will impact Mars in October 2014. Also, let us assume that we want to demonstrate a nuclear disruption mission that would have enough dispersion time for the debris to disperse before Mars encounter.

From the information available for the comet 2013 A1 and the requirements set on mission to impact the comet and allow time for dispersion of the debris before the anticipated date of its Mars encounter, an established timeline from January of 2013 to October of 2014 has been set for the AMiDST. During this time, spacecraft would have to be launched, intercept the target, and allow time for the disrupted body to disperse. To help visualize this established launch window, Figure 4 shows the corresponding ΔV for a given launch date and mission duration.

From previously studied missions to other NEOs, the feasible mission ΔV were generally less than 7 km/s. If this is taken to be true for this comet as well, then the mission launch window becomes rather small, with mission durations of about 200 days or more.

Obviously, the best mission would require the smallest amount of ΔV , which would imply that a given launch vehicle could lift more mass into orbit, so the limitation of total ΔV previously discussed is not really a constraint as much as an interesting bit of information to keep in mind during the design process. The important constraints that will limit the mission feasibility window are the launch date and mission duration resulting in an impact date that allows for dispersion of the disrupted debris. So, the launch date cannot occur before the discovery date, meaning that the departure date cannot be before January 3, 2013. Taking a pretty relaxed approach to the mission constraints, let the minimum dispersion time be at least 15 days and the maximum flight time be a year. The optimal mission parameters for an impact mission to comet 2013 A1 are shown in Table 2.

The resulting optimal mission parameters that meet the established constraints show a departure date a little more than eight months after discovery and a year long mission flight time, requiring a departure ΔV of just under four kilometers per second. After the year long transit from Earth to comet 2013 A1, the spacecraft would impact the comet about 65 days before the expected close approach with Mars. Using these parameters as the basis for an impact mission to comet 2013 A1, the resulting mission design parameters are summarized in Table 3. The design of the

Table 2. Optimal constrained mission parameters for an impact mission to comet 2013 A1.

Parameter	Value
Departure Date	August 15, 2013
Flight Time (days)	365
Departure ΔV (km/s)	3.963
Dispersion time (days)	65

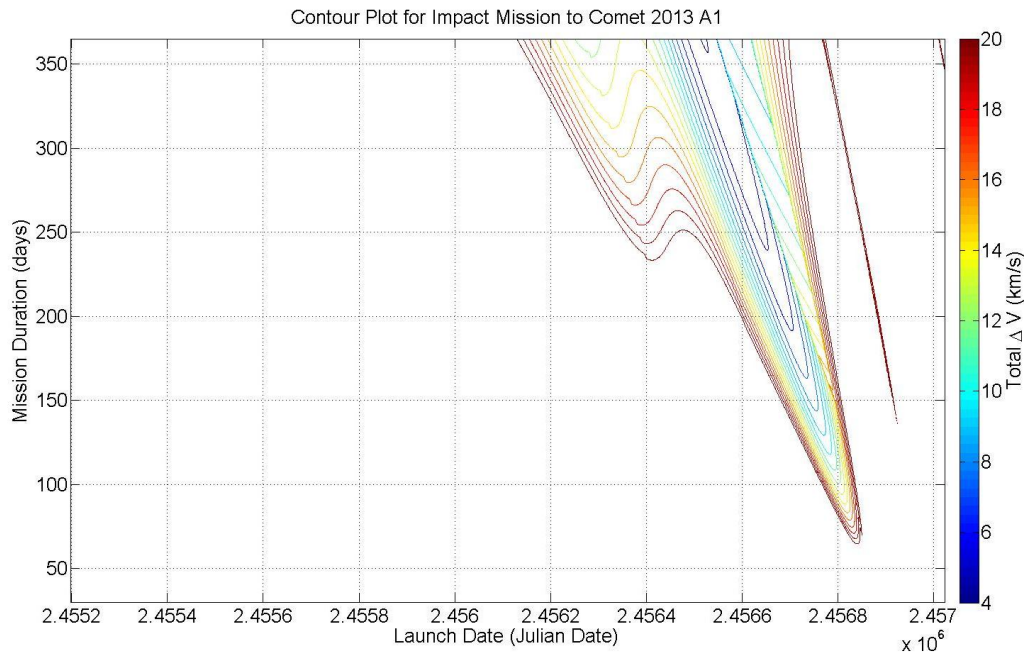


Figure 4. Contour plot showing total mission ΔV based on launch date and mission flight time. The departure dates are from January 2010 to January 2015, and mission durations vary from 30 days to one year.

Table 3. Mission design parameters for intercept mission to comet 2013 A1.

Mission Parameter	Value
Comet	2013 A1
LEO altitude (km)	185
Spacecraft Designation	HAIV
Total HAIV Mass (kg)	1800
Departure ΔV (km/s)	3.96
C3 (km^2/s^2)	16.74
Launch Vehicle	Delta IV Medium
Departure Date	August 15, 2013
Mission Duration (days)	365
Arrival Angle (deg)	85.2
Impact Velocity (km/s)	35.1
Arrival Date	August 15, 2014
Estimated Mission Cost (\$)	842M

launched spacecraft is based upon the ADRC's two-body HAIV. Assuming the total mass of the spacecraft is 1800 kg, the smallest launch vehicle that can place the HAIV into an interplanetary orbit with C3 of $16.74 \text{ km}^2/\text{s}^2$ necessary to meet the comet is the Delta IV Medium. Given that the Delta IV class launch vehicles have been decommissioned, the smallest Atlas V launch vehicle (Atlas V 401) could be used to complete the mission. The Atlas V 401 is a larger rocket than the Delta IV Medium, so it would be too powerful given this mission architecture, but it would do the job just as well.

Upon arriving at comet 2013 A1, on August 15, 2014, the spacecraft would have a relative impact speed of over 35 km/s at an impact angle of about 85.3° . Meaning that the comet and the spacecraft's velocity vectors, at the time of impact, would be nearly perpendicular to each other. Depending on whether or not such an impact would be desirable or not, trajectory correction maneuvers could perhaps be applied to have an impact that is more along the line of the

asteroid's velocity vector. To gain a visual of what the transfer orbit from Earth to the comet would look like, Figure 5 shows the orbits of the Earth, 2013 A1, and the spacecraft, in green, blue, and red respectively, in the Earth's orbital plane.

This two dimensional representation of the orbits does not show a lot of information about the comet or spacecraft's orbits, given that the comet has a highly inclined orbit with respect to the ecliptic. Looking at a three dimensional representation of the orbits tells a better story (Figure 6).

It can be seen that the comet's orbit (blue) is traveling up toward the ecliptic, and the spacecraft's orbit has to travel below the ecliptic to meet it before it crosses the ecliptic, and Mars. Once the HAIV impacts 2013 A1, there will be 65 days for the disrupted comet debris to disperse before its encounter with Mars.

An important point to make note of in the mission design for this particular body is the mission flight time. The mission duration tends to reach the upper bound, where given the other constraints of this problem tend to have lower changes in velocity. In other words, the more tightly the mission duration is bound the larger the total mission ΔV becomes, the more likely the missions are to be infeasible.

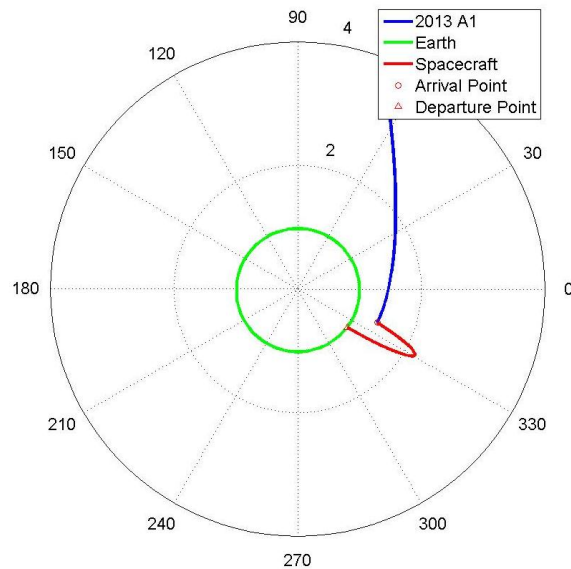


Figure 5. Two-dimensional depiction of the spacecraft's orbit trajectory from Earth to intercept comet 2013 A1.

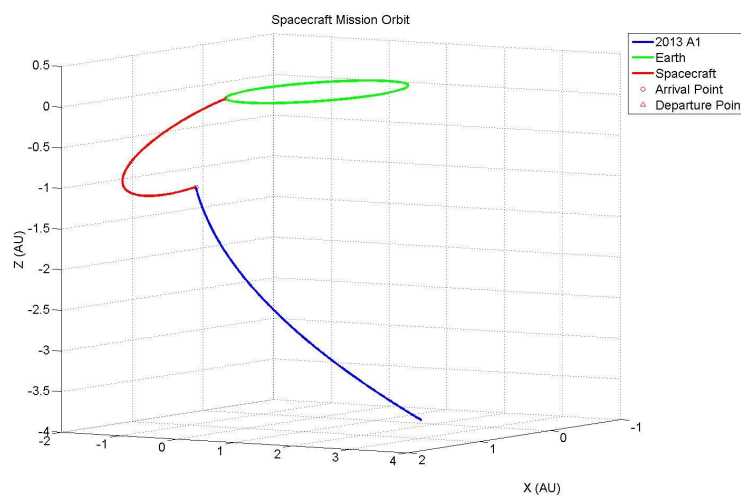


Figure 6. Three-dimensional depiction of the spacecraft's orbit trajectory from Earth to intercept comet 2013 A1.

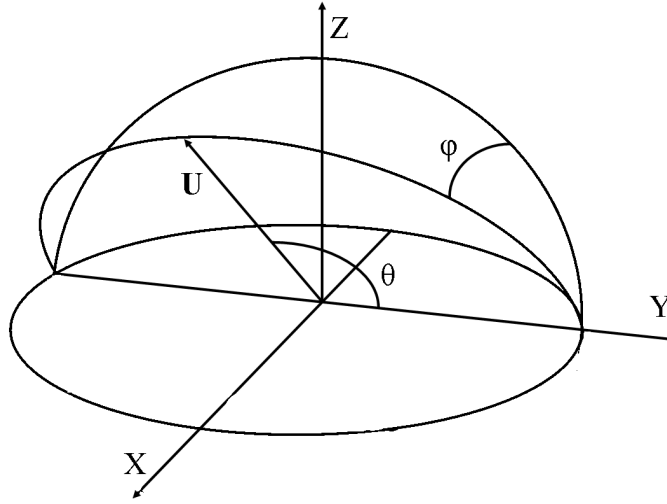


Figure 7. Reference frame of \vec{U} . The origin is placed at the planet's center, the positive x-axis is opposite the direction of the Sun, the y-axis is in the direction of the planet's motion, and the z-axis is parallel to the planet's angular momentum vector. The angles ϕ and θ define the direction of \vec{U} .

III. Keyholes for Planetary Mission Design

When a body undergoes an encounter with a planet, there are a number ways that its orbit will be affected. The environment around a planet is very dynamic in nature, and small inaccuracies in modeling can result in drastic differences between the simulated trajectories and the actual trajectory. Getting a good understanding behind the geometry of planetary close-approaches and the effect that they have on the orbital elements of the bodies that undergo them should assist with the task of predicting the resulting orbital trajectory after a close flyby of a planet. In some cases, upon having a close approach with a planet the asteroid will pass through what is called a gravitational keyhole. As will be discussed later in this paper, asteroid 2013 PDC-E ends up having a close-encounter with the Earth and travels through a keyhole in its encounter target plane. A brief description of analytic keyhole theory is provided in the Appendix, but for now we will discuss the variation in orbital elements due to planetary close-encounters.

III.A. Basic Assumptions

The dynamical system under consideration in the following analysis consists of the Sun, a planet orbiting the Sun on a circular orbit, and an asteroid, viewed as a particle, that is on an eccentric and inclined orbit around the Sun that crosses the orbit of the planet. Assume the planet has an orbital radius $R = 1$, the product $k\sqrt{M} = 1$, where k is the Gaussian constant and M is the mass of the Sun, and the asteroid has orbital parameters $(a, e, i, \omega, \Omega)$. In order to have the asteroid cross the orbital path of the planet, the asteroid must meet the following criteria: $a(1 - e) < 1 < a(1 + e)$. The frame of reference established for this analysis is centered on the planet, the x -axis points radially opposite to the Sun, the y -axis is the direction of motion of the planet itself, and the z -axis is completes the right-handed system by pointing in the direction of the planet's angular momentum vector. The three most important orbital elements used in the analysis are the semi-major axis a , the eccentricity e , and the inclination i .

III.B. Relationship Between Orbital Parameters a, e, i and U, ϕ, θ

Let $\mathbf{U} = (U_x, U_y, U_z)$ and U be the relative velocity vector and magnitude between the planet and the asteroid [13], defined as

$$U = \sqrt{3 - \left[\frac{1}{a} + 2\sqrt{a(1 - e^2)} \cos i \right]} \quad (4)$$

$$U_x = U \sin \theta \sin \phi \quad (5)$$

$$U_y = U \cos \theta \quad (6)$$

$$U_z = U \sin \theta \cos \phi \quad (7)$$

where θ and ϕ define the angles that define the direction of U by

$$\phi = \tan^{-1} \left[\pm \sqrt{\frac{2a-1}{a^2(1-e^2)}} - 1 \frac{1}{\sin i} \right] \quad (8)$$

$$\theta = \cos^{-1} \left[\frac{1-U^2-1/a}{2U} \right] \quad (9)$$

where θ may vary between 0 and π , and ϕ between $-\pi/2$ and $\pi/2$.

In terms of a , e , and i , the components of \mathbf{U} are given by

$$U_x = \left[2 - \frac{1}{a} - a(1-e^2) \right]^{1/2} \quad (10)$$

$$U_y = \sqrt{a(1-e^2)} \cos i - 1 \quad (11)$$

$$U_z = \sqrt{a(1-e^2)} \sin i \quad (12)$$

and, inversely, we have

$$a = \frac{1}{1-U^2-2U_y} \quad (13)$$

$$e = [U^4 + 4U_y^2 + U_x^2(1-U^2-2U_y) + 4U^2U_y]^{1/2} \quad (14)$$

$$i = \sin^{-1} \sqrt{U_z^2/[U_x^2 + (1+U_y)^2]} \quad (15)$$

III.C. Post-Keyhole Geometry

After the asteroid has an encounter with the target planet, the \mathbf{U} vector is rotated by an angle γ in the direction ψ , where ψ is the angle measured counter-clockwise from the meridian containing the \mathbf{U} vector. The deflection angle γ is related to the encounter parameter b by

$$\tan \frac{1}{2}\gamma = \frac{m}{bU^2} \quad (16)$$

where m is the mass of the planet, in units of the Sun's mass. The angle θ after the encounter, denoted by θ' , is calculated from

$$\cos \theta' = \cos \theta \cos \gamma + \sin \theta \sin \gamma \cos \psi \quad (17)$$

and, defining $\xi = \phi - \phi'$, we have

$$\sin \xi = \sin \psi \sin \gamma / \sin \theta' \quad (18)$$

$$\cos \xi = (\cos \gamma \sin \theta - \sin \gamma \cos \theta \cos \psi) / \sin \theta' \quad (19)$$

$$\tan \xi = \sin \psi \sin \gamma / (\cos \gamma \sin \theta - \sin \gamma \cos \theta \cos \psi) \quad (20)$$

$$\tan \phi' = (\tan \phi - \tan \xi) / (1 + \tan \phi \tan \xi) \quad (21)$$

Evaluating for the post-encounter variables θ' and ϕ' , the values of a' , e' , and i' can be obtained accordingly [13].

III.D. Post-Keyhole Orbital Elements

In the case of asteroid 2013 PDC-E, the post-encounter orbital elements were given in addition to the pre-encounter elements, so an analysis of the post-encounter geometry is not needed. However, the scenario lends itself well as a learning exercise to show how the approach and post-encounter geometries relate to each other in the context of an Earth-threatening asteroid. The important orbital parameters to the analysis are given in Table 4.

III.D.1. Post-Keyhole Semi-major Axis

Given that $|\mathbf{U}|$ is constant, the variation in the semi-major axis Δa depends only on the parameters θ and θ' as

$$\Delta a = \frac{a' - a}{a} = \frac{1 - U^2 - 2U \cos \theta}{1 - U^2 - 2U \cos \theta'} - 1 \quad (22)$$

Table 4. Orbital elements of asteroid 2013 PDC-E for pre-keyhole and post-keyhole.

	Pre-Keyhole	Post-Keyhole
a	0.9846	1.1616
e	0.18831	0.22537
i	1.3941°	1.5311°

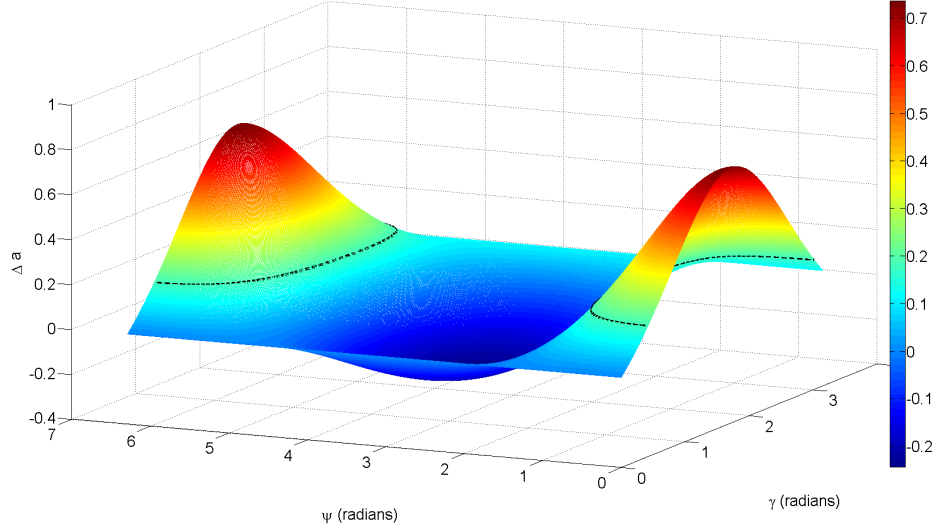


Figure 8. Surface plot of variation of semi-major axis for asteroid 2013 PDC-E.

Figure 8 shows the variation in the semi-major axis a . The colors on the mesh depict the value of the variation, and the black dotted line depicts the resulting semi-major axis variation of 2013 PDC-E from its Earth encounter. From the figure, it can be seen that the asteroid is susceptible to having its semi-major axis increased or decreased, depending on the values of γ and ψ . Preliminary observations show that values of ψ between about $\pi/2$ and $3\pi/2$ will cause 2013 PDC-E to have a smaller post-encounter semi-major axis than its pre-encounter value. In this particular case, the change in semi-major axis is about 0.18 meaning that the value of ψ will come about to be smaller than $\pi/2$ or greater than $3\pi/2$.

III.D.2. Post-Keyhole Inclination

The tangent of inclination is defined as

$$\tan i = \frac{\cos \phi \sin \theta}{1/U + \cos \theta} = \frac{U_z}{1 + U_y} \quad (23)$$

and after the rotation of the relative velocity vector by the deflection angle γ in the direction of ψ , it becomes

$$\tan i' = \frac{\cos \phi \sin \theta \cos \gamma - \cos \phi \cos \theta \sin \gamma \cos \psi + \sin \phi \sin \gamma \sin \psi}{1/U + \cos \theta \cos \gamma + \sin \theta \sin \gamma \cos \psi} \quad (24)$$

The variation in inclination can be described by $\Delta i = \tan i' - \tan i$ [13]. Figure 9 depicts the variation of the inclination of the orbits of asteroid 2013 PDC-E. The black dotted line on the meshed grid shows the resulting variation of the inclination after the encounter with the Earth. The plot of post-encounter inclination variation has two distinct sections to it. When ψ is less than π the post-encounter inclination would be greater than the pre-encounter inclination, and when ψ is greater than π the inclination would decrease. The largest change in inclination seems to occur at ψ values of $\pi/2$ and $3\pi/2$.

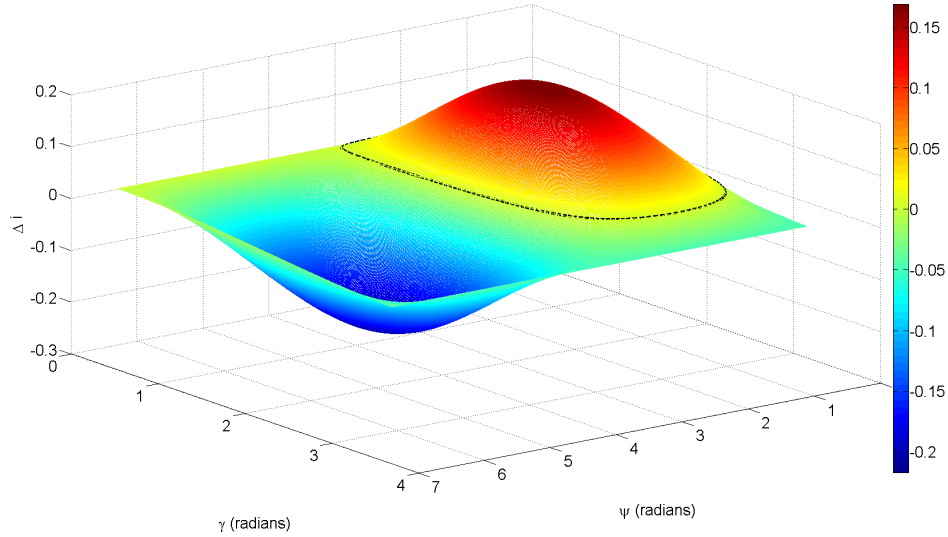


Figure 9. Surface plot of variation of inclination for asteroid 2013 PDC-E.

III.D.3. Post-Keyhole Eccentricity

Recalling that

$$e^2 = U^4 + 4U_y^2 + U_x^2(1 - U^2 - 2U_y) + 4U^2U_y \quad (25)$$

the expression for the pre-encounter eccentricity of the asteroid orbit can be expressed in terms of the relative velocity magnitude and its components. Making a substitution for the corresponding post-encounter terms, the value of the eccentricity after the encounter with the target planet can be calculated as

$$e = \sqrt{U'^4 + 4U_y'^2 + U_x'^2(1 - U'^2 - 2U_y') + 4U'^2U_y'} \quad (26)$$

Taking the difference between the post- and pre-encounter eccentricities shows the variation in the orbital eccentricity ($\Delta e = e' - e$) based on the planetary encounter. Figure 10 depicts the variation of the eccentricity of asteroid 2013 PDC-E. The black dotted lines shown in the figure indicate the level of variation between the pre- and post-encounter eccentricities of the asteroid. The plot of eccentricity variation has a bit more complicated structure for this asteroid than semi-major axis or inclination. Asteroid 2013 PDC-E would have more eccentric post-encounter orbits for values of ψ that approach the ends of the feasible domain $[0, 2\pi]$ and values near π . Values of ψ near $\pi/2$ and $3\pi/2$ seem to have a negative effect on the orbital eccentricities of the body.

A closer look at the variation equations of $(\Delta a, \Delta i, \Delta e)$ reveals cases where these equations can be further simplified, or interesting results become more apparent. Such an analysis is omitted in this paper. As is, this analysis only enables us to understand the potential variations in the orbital elements of a body having an encounter with the planet, to get a firm grasp of the exact variation in the orbital elements would require either an analytic analysis of the encounter or a numerical approach to find the ψ and γ values.

IV. Fictional Mission Design for Asteroid 2013 PDC-E

In April 2013, the 2013 IAA Planetary Defense Conference was held in Flagstaff, AZ, USA. As a part of the conference, there was a time set aside for a dedicated Mitigation Response and Disaster Management Exercise where a fictitious asteroid named 2013 PDC-E was revealed to be on a potential impact trajectory with Earth. This 300-m asteroid was expected to have a close encounter with the Earth on November 22, 2023 where it may impact the planet or pass through a keyhole to then impact the planet later in the future. As the exercise progressed, the participants were informed that the asteroid would not impact the Earth in 2023, but instead would pass through a keyhole that would set it into a resonance orbit with the Earth that would result in an Earth impact on November 29, 2028. The purpose of the exercise was to entertain the idea of an Earth-threatening asteroid and simulate the reaction of the participants fulfilling roles ranging from characterization of the object, mitigation techniques, the United Nations, and the general

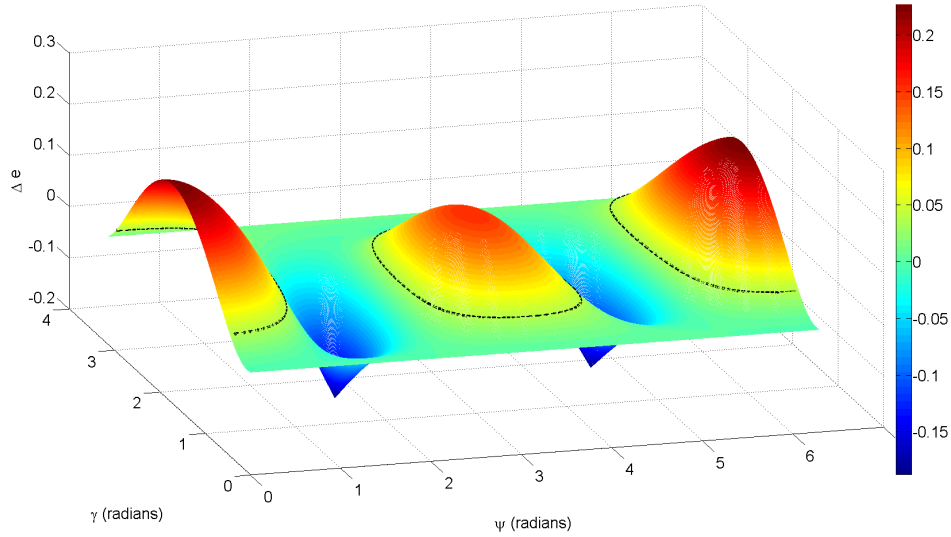


Figure 10. Surface plot of variation of eccentricity for asteroid 2013 PDC-E.

public. This section will go through hypothetical mission scenarios using pre- and post-keyhole data of the asteroid, as well as an analysis of the asteroid's encounter characteristics.

IV.A. Pre-Keyhole Mission Designs

On a trajectory to have a close-encounter with Earth, asteroid 2013 PDC-E was discovered early enough where, if we assume that we are launch capable at the time of discovery, deflection/disruption missions could be launched prior to the encounter date. In order to diminish the threat to the Earth, disruption missions will be entertained to attempt to destroy or at least deflect the asteroid from its current trajectory to avoid impacting the planet and/or the keyhole on the resulting target plane. Two mission types will be explored for this pre-keyhole trajectory: (i) short mission duration with a long dispersion time and (ii) long mission duration with a long dispersion time. Given the danger that the asteroid poses to Earth, there should exist plenty of opportunities to launch spacecraft to the body - especially closer to the encounter date. The porkchop plot for missions to the asteroid, pre-2023 encounter shown in Figure 11 agree with this assessment. Missions with short dispersion times are not considered in this part of the analysis since the result is to allow for the asteroid time to miss the Earth and the keyhole on its encounter, short deflection times would not allow for effective perturbation of the asteroid.

IV.A.1. Short-Duration, Long-Dispersion, Pre-Keyhole Mission

Launching a mission with a short mission duration and a long deflection time before encounter should result in a minimal ΔV mission that would allow plenty of time for the fragmented asteroid to avoid the important areas of the target plane (i.e. the Earth and the gravitational keyhole). For this mission type, the upper bound for the mission duration will be set for 60 days and the dispersion time will be set for anything between 200 days and 7 years. With such a wide range for the dispersion time, the best solution should tend to lean towards the upper bound. Assuming a spacecraft mass of 2,000 kilograms, the locally optimal mission design parameters are shown in Table 5.

Table 5. Optimal constrained mission parameters for a short-duration, long-dispersion pre-keyhole mission to asteroid 2013 PDC-E.

Parameter	Value
Departure Date	April 6, 2019
Flight Time (days)	60
Departure ΔV (km/s)	3.34
Dispersion time (days)	1631

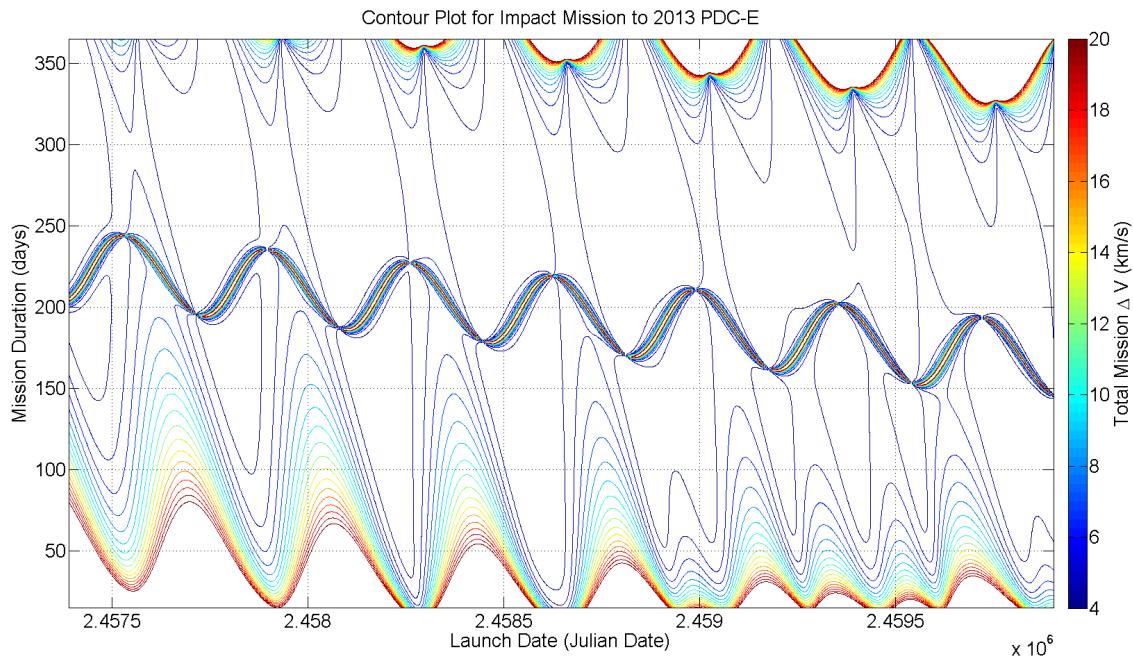


Figure 11. Mission contour plot of total ΔV in terms of launch date and mission flight time for the pre-encounter trajectory of asteroid 2013 PDC-E.

Table 6. Mission design parameters for a short-duration, long-dispersion pre-keyhole intercept mission to asteroid 2013 PDC-E.

Mission Parameter	Value
Asteroid	2013 PDC-E
LEO altitude (km)	185
Spacecraft Designation	Kinetic Impactor
Total HAIV Mass (kg)	2000
Departure ΔV (km/s)	3.34
C3 (km^2/s^2)	2.64
Launch Vehicle	Delta IV Medium
Departure Date	April 6, 2019
Mission Duration (days)	60
Arrival Angle (deg)	12.2
Impact Velocity (km/s)	6.52
Arrival Date	June 5, 2019
Estimated Mission Cost (\$)	904M

For these mission parameters, the preliminary mission design result is provided in Table 6. The resulting mission has a low C3 of about $2.64 \text{ km}^2/\text{s}^2$, meaning that with a spacecraft mass of 2,000 kg, most launch vehicles would be capable of injecting the spacecraft into the desired impact trajectory - in this case a Delta IV Medium would be the smallest of those launch vehicles. An impact in June 2019 leaves about four and a half years for the impact to effect asteroid. The relatively high speed at which the spacecraft would impact the asteroid and the amount of dispersion time there would be before its Earth impact seems to imply that a kinetic impactor spacecraft may be sufficient enough to perturb the asteroid from an Earth impacting or resonance orbit trajectory upon its 2023 encounter. In the case that the mission would prove unsuccessful, there would be time to launch another mission to either try and perturb the asteroid more or disrupt it before encounter.

IV.A.2. Long-Duration, Long-Dispersion, Pre-Keyhole Mission

While the ΔV in the short-duration, long-dispersion mission is not very large that is likely due to the wide range of dispersion time allowed. However, that change in velocity can probably be brought down a little more if a longer mission duration is allowed. So, for this particular analysis the dispersion time range is kept the same (200 days to about seven years), but the mission duration is allowed to take up to a year instead of two months. Looser constraints such as these should result in a cheaper mission, in terms of ΔV . Once again assuming a spacecraft mass of 2,000 kg, the optimized mission design variables for this particular scenario are presented in Table 7.

Table 7. Optimal constrained mission parameters for a long-duration, long-dispersion pre-keyhole mission to asteroid 2013 PDC-E.

Parameter	Value
Departure Date	January 5, 2022
Flight Time (days)	328
Departure ΔV (km/s)	3.23
Dispersion time (days)	358

Interestingly, widening the range of mission durations results in a mission that does have a longer flight time with a lower ΔV , but the dispersion time drops considerably to a little less than a year. There are many other solutions that fit the criteria and have longer dispersion times. However, since the single over-arching criteria to determine the optimal mission design given the constrained parameters is mission ΔV , this smaller dispersion time mission is the better mission design by AMiDST. The design result for these mission parameters is provided in Table 8.

Table 8. Mission design parameters for a long-duration, long-dispersion pre-keyhole intercept mission to asteroid 2013 PDC-E.

Mission Parameter	Value
Asteroid	2013 PDC-E
LEO altitude (km)	185
Spacecraft Designation	HAIV
NED mass (kg)	300
Total HAIV Mass (kg)	2000
Departure ΔV (km/s)	3.23
C3 (km^2/s^2)	0.043
Launch Vehicle	Delta IV Medium
Departure Date	January 5, 2022
Mission Duration (days)	328
Arrival Angle (deg)	9.77
Impact Velocity (km/s)	5.12
Arrival Date	November 29, 2022
Estimated Mission Cost (\$)	811M

Despite the low C3 orbit that would be required to put the spacecraft into an impacting trajectory with 2013 PDC-E, the impact would be between the spacecraft and the asteroid still be in the hypervelocity regime. This would imply that while the preferred spacecraft configuration would be a kinetic impactor due to the high speed impact, the HAIV concept would serve as a better alternative due to the shortened dispersion time before encounter [7,8]. Also, it is interesting to note that the total cost of the mission dropped a little bit despite the fact that the same launch vehicle can be used for both missions. The reason for this is that the mass of the NED is not used in the calculation of the spacecraft cost. The mission orbit is shown in Figure 12. Given the small C3 orbit that the launch vehicle would place the spacecraft into, it makes sense that the spacecraft would essentially enter into an Earth-trailing orbit that would impact the asteroid after the Earth has passed the intersection between the asteroid's and its own orbit.

While attempting to deflect/disrupt a hazardous object before its close-encounter with the Earth is a rather aggressive approach to planetary defense, the two types of mission designs presented here are a bit on the conservative end of the spectrum. The missions are relatively low risk in the sense that if the spacecraft were a kinetic impactor they would not impart very much ΔV to the asteroid and could be deemed a demonstration of our ability to intercept the body,

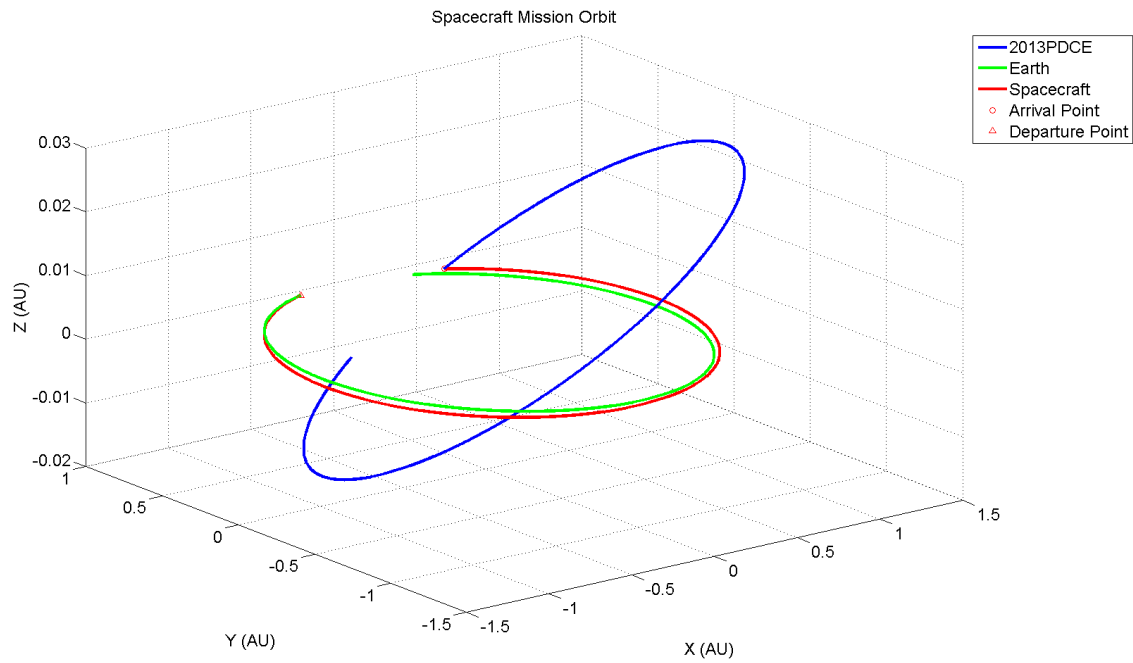


Figure 12. Mission orbit diagram for a long-duration, long-dispersion pre-keyhole mission to asteroid 2013 PDC-E before its planetary encounter in 2023.

and using a HAIV concept spacecraft could result in the same end goal or could attempt at nullifying the threat early before any real danger arose. The following mission designs for the post-encounter asteroid trajectory are much more aggressive given that the end result would be complete disruption of asteroid 2013 PDC-E.

IV.B. Post-Keyhole Mission Designs

Upon its encounter with the Earth, 2013 PDC-E passes through a keyhole on the 2023 target plane. The resulting asteroid trajectory has a 4:5 resonance with the Earth, meaning that the asteroid will impact the Earth after four of its own orbits and five of the Earth's. To deal with the certain threat to the Earth, four fictional mission types will be discussed as potential mission scenarios: (i) long-duration, long-dispersion, (ii) short-duration, long-dispersion, (iii) long-duration, short-dispersion, and (iv) short-duration, short dispersion. The purpose of these missions would be to disrupt the asteroid, given that five years may not be enough time to perturb the asteroid enough to avoid a collision with the Earth, in hopes to fragment the asteroid to the point that the damage on the ground would be minimal or not at all. In order to fragment the asteroid, the HAIV spacecraft will have a total mass of 3,500 kg containing a 1,000-kg NED.

Observing the porkchop plot for the post-keyhole trajectory of asteroid 2013 PDC-E, there is a striking difference to the contour map of the pre-keyhole trajectory. While the pre-keyhole contour shows small regions throughout the launch date domain (around 200-day mission durations) that would likely result in infeasible mission designs, the post-keyhole contour has entire regions where the required mission ΔV is high enough that it is easy to see that any mission from that region would be infeasible. On the other hand, like the pre-keyhole contour map, there are clearly evident regions where missions should be relatively easy to construct - particularly those close to the encounter date in 2023 and the anticipated impact date in 2028.

IV.B.1. Long-Duration, Long-Dispersion, Post-Keyhole Mission

Prioritizing lower ΔV with longer dispersion times and long mission durations should result in very feasible missions for 2013 PDC-E. The only real constraint for this particular scenario is on the dispersion time, the spacecraft must impact the asteroid at least 200 days before the expected impact date. Given this relatively unconstrained situation, the optimal mission parameters for a long-term, long-dispersion mission are shown in Table 9.

The mission flight time comes out to be 318 days from the launch date of December 27, 2023, resulting in an impact date of November 9, 2024 and a dispersion time of a little over four years.

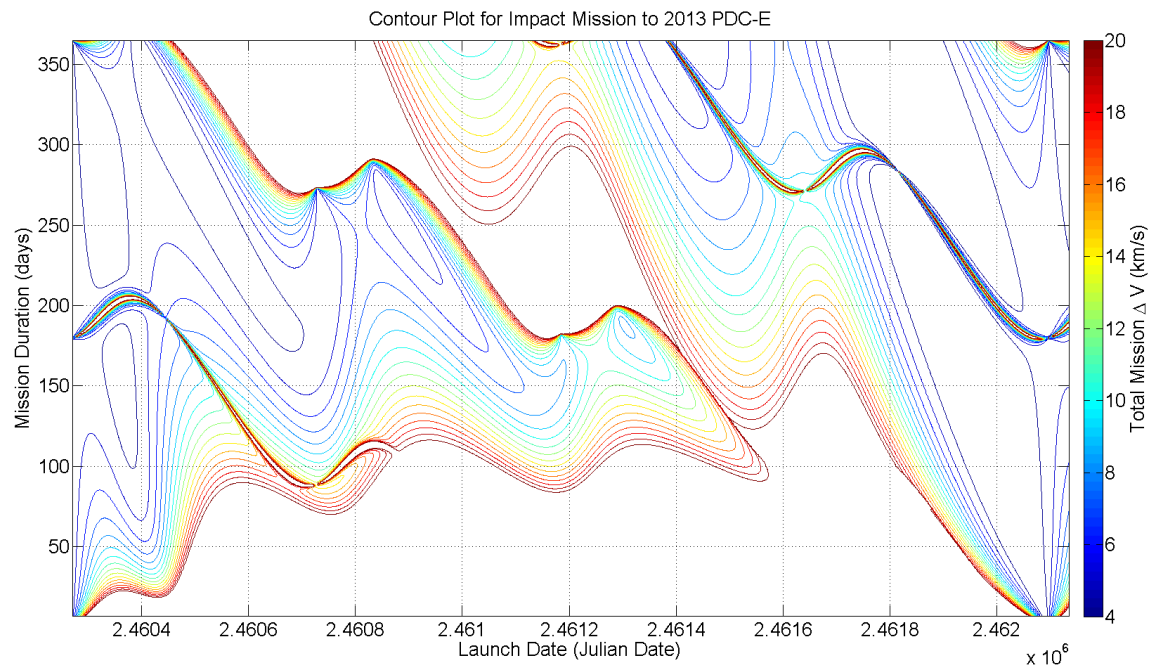


Figure 13. Mission contour plot of total ΔV in terms of launch date and mission flight time for the post-keyhole trajectory of asteroid 2013 PDC-E.

Using the parameters from Table 9, a complete mission design with a 3,500-kg HAIV spacecraft can be performed. The hyperbolic orbit that the spacecraft would be placed into has a C3 value of about $3.32 \text{ km}^2/\text{s}^2$, and a Delta IV M+(4,2) is the smallest launch vehicle with the capability to lift the spacecraft into its impacting trajectory.

Upon arriving at the asteroid, the spacecraft would have a relative impact velocity of about 1.5 km/s and arrival angle of a little more than 3.5 degrees. A mission orbit is shown in Figure 14.

The blue trajectory is that of the asteroid, green is the Earth's trajectory and the red trajectory shows the spacecraft's path from launch at Earth to impact with the asteroid. With such a relatively low impact velocity, the only way to protect the Earth from the asteroid threat would be the energy from the detonation of the NED used to fracture the asteroid. The estimated mission cost is just over a billion dollars, mostly due to the mass of the HAIV spacecraft.

IV.B.2. Short-Duration, Long-Dispersion, Post-Keyhole Mission

Rating the length of dispersion time as a more important design parameter than the mission duration would result in a short-term, long-dispersion mission to asteroid 2013 PDC-E. For this scenario, the mission duration is limited to 60 days or less and the dispersion time is still bounded between 200 days and five years.

Interestingly enough, by minimizing the mission ΔV , given the previously mentioned constraints on the mission duration and dispersion time variables, the resulting optimal mission design would have a launch date of November 22, 2023 - the keyhole encounter date. The spacecraft would have to be ready to launch with virtually no time to analyze the post-keyhole orbit. In addition to the encounter-date launch date, minimizing ΔV results in mission duration of seven years, almost five years of dispersion time to the anticipated impact date. The associated departure velocity from low-Earth orbit is considerably larger than the long-duration, long-dispersion mission counterpart.

Table 9. Optimal constrained mission parameters for a long-duration, long-dispersion post-keyhole mission to asteroid 2013 PDC-E.

Parameter	Value
Departure Date	December 27, 2023
Flight Time (days)	318
Departure ΔV (km/s)	3.37
Dispersion time (days)	1473

Table 10. Mission design parameters for a long-duration, long-dispersion post-keyhole intercept mission to asteroid 2013 PDC-E.

Mission Parameter	Value
Asteroid	2013 PDC-E
LEO altitude (km)	185
Spacecraft Designation	HAIV
NED Mass (kg)	1000
Total HAIV Mass (kg)	3500
Departure ΔV (km/s)	3.37
C3 (km^2/s^2)	3.32
Launch Vehicle	Delta IV M+(4,2)
Departure Date	December 27, 2023
Mission Duration (days)	318
Arrival Angle (deg)	3.52
Impact Velocity (km/s)	1.48
Arrival Date	November 9, 2024
Estimated Mission Cost (\$)	1,068M

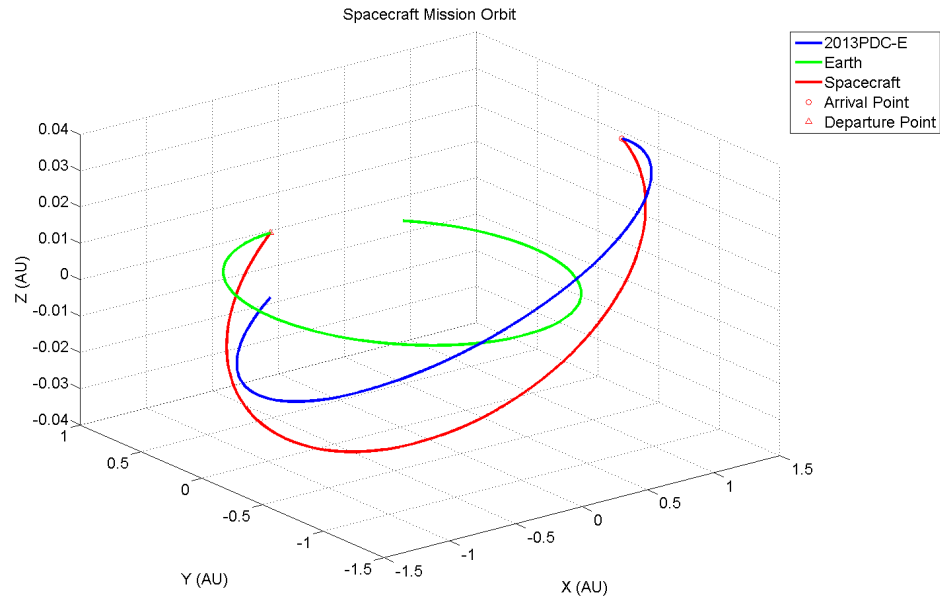


Figure 14. Mission orbit diagram for a long-duration, long-dispersion post-keyhole mission to asteroid 2013 PDC-E after its 2023 encounter.

Table 11. Optimal constrained mission parameters for a short-duration, long-dispersion post-keyhole mission to asteroid 2013 PDC-E.

Parameter	Value
Departure Date	November 22, 2023
Flight Time (days)	7
Departure ΔV (km/s)	4.42
Dispersion time (days)	1819

With the optimized mission parameters given in Table 11, the corresponding mission design variables are provided in Table 12. The C3 orbit required to put the spacecraft on its impact trajectory with asteroid 2013 PDC-E is very energetic and could be accomplished using an Atlas V 431 launch vehicle. However, despite the large-C3 hyperbolic orbit the spacecraft's relative impact velocity with the asteroid is very small, about 0.35 km/s, and a very shallow impact angle of less than 0.4 degrees. The estimated mission cost is almost 1.1 billion dollars, with the difference in cost between this scenario and the long-term, long-dispersion mission coming from the larger launch vehicle being used in this mission design.

Table 12. Mission design parameters for a short-duration, long-dispersion post-keyhole intercept mission to asteroid 2013 PDC-E.

Mission Parameter	Value
Asteroid	2013 PDC-E
LEO altitude (km)	185
Spacecraft Designation	HAIV
NED Mass (kg)	1000
Total HAIV Mass (kg)	3500
Departure ΔV (km/s)	4.42
C3 (km^2/s^2)	27.7
Launch Vehicle	Atlas V 431
Departure Date	November 22, 2023
Mission Duration (days)	7
Arrival Angle (deg)	0.39
Impact Velocity (km/s)	0.34
Arrival Date	November 9, 2024
Estimated Mission Cost (\$)	1,088M

IV.B.3. Long-Duration, Short-Dispersion, Post-Keyhole Mission

With the completion of the long-dispersion missions, the missions transition into the time frames where the impact date is not too far down the road and the missions become more and more last-minute scenarios. For this mission design, the mission duration is allowed to go as high as a year but the dispersion time is limited between seven and 30 days. Again, minimizing the mission ΔV within the field of potential candidate missions that fit the given criteria, the mission parameters from Table 13 are found. Leaving just eight days for the disrupted asteroid fragments to disperse, the identified mission would have a launch date of May 23, 2028 and a mission duration of 174 days.

Table 13. Optimal constrained mission parameters for a long-duration, short-dispersion post-keyhole mission to asteroid 2013 PDC-E.

Parameter	Value
Departure Date	May 23, 2028
Flight Time (days)	174
Departure ΔV (km/s)	3.23
Dispersion time (days)	8

The overall mission architecture is described in Table 14.

As was previously mentioned, the mission only allows for eight days of dispersion time with the arrival date of the spacecraft being on November 13, 2028. The impact angle between the spacecraft and the asteroid is not quite 11 degrees, with a relative impact speed of over six kilometers per second. This shallow, high speed impact makes sense considering the C3 orbit required for this mission barely exceeds $0.1 \text{ km}^2/\text{s}^2$ and at the time of intercept the asteroid is making its approach on Earth, Figure 15 shows the trajectories of the Earth, asteroid, and spacecraft in green, blue and red, respectively.

Table 14. Mission design parameters for a long-duration, short-dispersion post-keyhole intercept mission to asteroid 2013 PDC-E.

Mission Parameter	Value
Asteroid	2013 PDC-E
LEO altitude (km)	185
Spacecraft Designation	HAIV
NED Mass (kg)	1000
Total HAIV Mass (kg)	3500
Departure ΔV (km/s)	3.23
C3 (km ² /s ²)	0.11
Launch Vehicle	Delta IV M+(4,2)
Departure Date	May 23, 2028
Mission Duration (days)	174
Arrival Angle (deg)	10.82
Impact Velocity (km/s)	6.0
Arrival Date	November 13, 2028
Estimated Mission Cost (\$)	1,068M

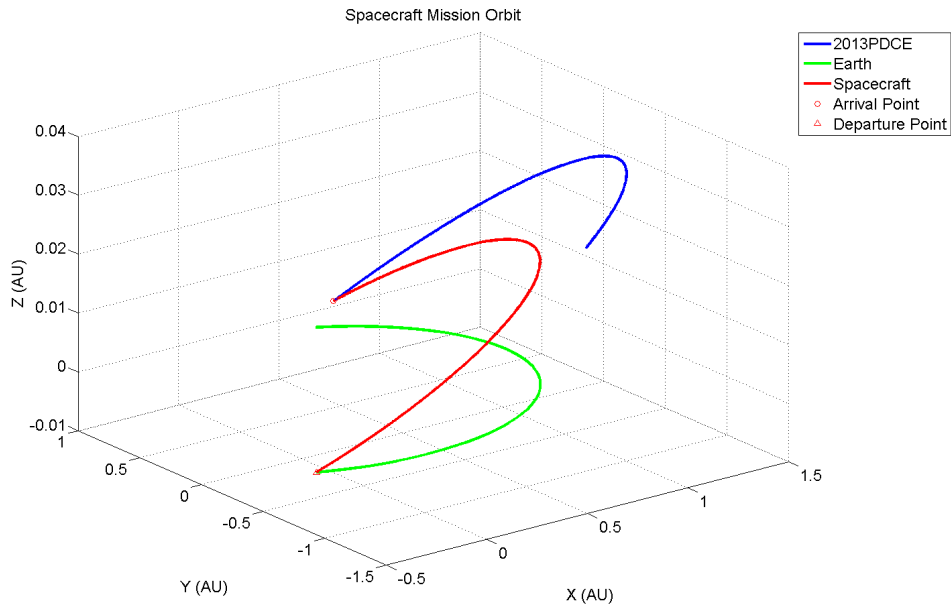


Figure 15. Mission orbit diagram for a long-duration, short-dispersion mission to asteroid 2013 PDC-E after its 2023 encounter.

IV.B.4. Short-Duration, Short-Dispersion, Post-Keyhole Mission

A short-term, short-dispersion mission is considered to be a last resort option for Earth, when time is of the essence and there are no options left. With a mission duration upper bound of 30 days and a dispersion time set to be between seven and 30 days, AMiDST deemed this mission design the easiest to complete with at most 2 months of warning. The selected mission has a flight time that runs into the upper bound of the allowable range, given that more mission flight time generally means lower mission ΔV . With only a slightly larger ΔV of about 3.318 km/s, this mission also results in a dispersion time of eight days after a 30-day cruise to the asteroid following an October-14-2028 launch date.

Table 15. Optimal constrained mission parameters for a short-duration, short-dispersion post-keyhole mission to asteroid 2013 PDC-E.

Parameter	Value
Departure Date	October 14, 2028
Flight Time (days)	30
Departure ΔV (km/s)	3.318
Dispersion time (days)	8

Table 16. Mission design parameters for a short-duration, short-dispersion post-keyhole intercept mission to asteroid 2013 PDC-E.

Mission Parameter	Value
Asteroid	2013 PDC-E
LEO altitude (km)	185
Spacecraft Designation	HAIV
NED Mass (kg)	1000
Total HAIV Mass (kg)	3500
Departure ΔV (km/s)	3.318
C3 (km ² /s ²)	2.0
Launch Vehicle	Delta IV M+(4,2)
Departure Date	October 14, 2028
Mission Duration (days)	30
Arrival Angle (deg)	13.5
Impact Velocity (km/s)	7.34
Arrival Date	November 13, 2028
Estimated Mission Cost (\$)	1,068M

The mission design parameters for this short-duration, short-dispersion mission, shown in Table 16, are not very different from those of the long-duration, short-dispersion mission discussed previously. An arrival angle of about 13.5° this time is only slightly larger than the previous 11°, and the relative impact speed increased a bit to over 7.3 km/s. Also, not surprisingly, the estimated mission costs for three of these four post-keyhole mission designs (long-duration/long-dispersion, long-duration/short-dispersion, short-duration/short-dispersion) have all been the same - given the size of the spacecraft has not changed and the desired launch vehicle is a Delta IV M+(4,2).

IV.C. Post-Keyhole Mission Design Summary

Each of the six missions analyzed in this section for hypothetical post-keyhole missions, with its own time and place, are completely feasible and would probably result in the salvation of the Earth. Making an attempt on the threatening body as early as possible would give some time afterwards in case something were to go wrong and/or the mission were to fail. But, this post-keyhole mission design assumed that we are ready to launch a spacecraft upon discovering a threat, if not, then this scenario is meaningless. If the basic assumption of launch readiness is taken as truth, then the best course of action for the asteroid 2013 PDC-E would have been to impact the asteroid long before its 2023 keyhole encounter with Earth - employing one of the first two mission designs. If there is hesitation towards that idea based on the potential of perturbing the asteroid into an Earth-impacting trajectory or resonant trajectory, then what may be

considered a more suitable course of action would be to allow the asteroid to have its encounter with the Earth and plan a mission based on its altered trajectory.

Planning a mission based on the altered orbit trajectory of 2013 PDC-E would mean that the first two of the post-keyhole mission designs would be under consideration. However, the short-duration, long-dispersion mission launching on the encounter date may be a little of an optimistic plan. There may not be enough time to analyze asteroid's new orbital trajectory to see if a disruption mission is even deemed necessary. If it is absolutely necessary and the time has grown short, the last option for mankind should be to launch a mission with a short-dispersion time (either of the last two mission designs). But, it cannot be stressed enough that that option should not be taken as the only plan of attack in hopes that new information would make the asteroid less of a threat - early action is best. Regardless, any action may be better than inaction.

V. Conclusion

After an introductory discussion of a fictional mission design for comet 2013 A1 (with no keyholes), performed using AMiDST, this paper presented the on-going research work at Asteroid Deflection Research Center on further developing a high-fidelity gravitational simulator and characterizing post-encounter orbital variations as applied to planetary defense mission design. As an example of Earth-impacting asteroids passing through keyholes, a fictitious asteroid 2013 PDC-E was used to demonstrate the effectiveness of using AMiDST for various pre-keyhole as well as post-keyhole mission designs.

Appendix: An Overview of Keyhole Theory

Target Planes

A target plane is defined as a geocentric plane oriented to be normal to the asteroid's geocentric velocity vector. By observing the point of intersection of an asteroid trajectory with the target plane can lend significant insight into the nature of a future encounter. In general, there are two distinct planes and several coordinate systems that can be used in such a framework. The classical target plane is referred to as the b-plane, which has been used in astrodynamics since the 1960's. The b-plane is oriented normal to the incoming asymptote of the geocentric hyperbola, or normal to the unperturbed relative velocity \vec{v}_∞ . The plane's name is a reference to the so-called impact parameter b , the distance from the geocenter to the intercept of the asymptote on this plane, known as the minimum encounter distance along the unperturbed trajectory [14]. Figure 16 depicts the relationship between the target b-plane and the trajectory plane of the asteroid. The system of coordinates that will be used for the analyses conducted in this paper are described later, those shown on the figure are just an example that could be used.

Target Plane Coordinates

Generally it is convention to place the origin of the b-plane's coordinate system at the geocenter, but the orientation of the coordinate axes on the plane is arbitrary. The system has been fixed at times by aligning the axes in a way so that one of the nominal target plane coordinates is zero, or by aligning one of the coordinate axes with either the projection of the Earth's polar axis or the projection of the Earth's heliocentric velocity.

One of the most important functions of the target plane is to determine whether a collision is possible, and if not, how deep the encounter will be. With the b-plane, we obtain the minimum distance of the unperturbed asteroid orbit at its closest approach point with the Earth - the impact parameter b . That single variable however does not tell whether the asteroid's perturbed trajectory will intersect the image of the Earth on the following encounter, but the information can be extracted by scaling the Earth radius R_\oplus according to the following relationship

$$b_\oplus = R_\oplus \sqrt{1 + \frac{v_e^2}{v_\infty^2}} \quad (27)$$

where v_e is the Earth escape velocity

$$v_e = \sqrt{\frac{2GM_\oplus}{R_\oplus}} \quad (28)$$

With this formulation a given trajectory impacts the Earth if $b < b_\oplus$, and would not otherwise. Alternatively, the impact parameter could be scaled while leaving the image of the Earth on the b-plane unchanged. The two scalings are

Resonant Returns and Keyholes

A resonant return orbit is a consequence of an encounter with Earth, such that the asteroid is perturbed into an orbit of period $P' \approx k/h$ years, with h and k integers. After h revolutions of the asteroid and k revolutions of the Earth, both bodies are in the same region of the first encounter, causing a second encounter between the asteroid and the Earth.

The analytic theory of resonant returns that has been developed by Valsecchi et al. [15] treats close encounters with an extension of Opik's theory, adding a Keplerian heliocentric propagation between the encounters. The heliocentric propagation establishes a link between the outcome of the first encounter and the initial conditions of the next one. During the Earth encounter, the motion of the asteroid is assumed to take place on one of the asymptotes of the encounter hyperbola. The asymptote is directed along the unperturbed geocentric encounter velocity \vec{v}_∞ , crosses the b-plane at a right angle, and the vector from the Earth to the intersection point is denoted by \vec{b} [14].

According to Opik's theory, the encounter of the asteroid with the Earth consists of the instantaneous transition, when the body reaches the b-plane, from the pre-encounter velocity vector \vec{v}_∞ to the post-encounter velocity vector \vec{v}'_∞ , such that $v'_\infty = v_\infty$. And, the angles θ' and ϕ' are simple functions of v_∞ , θ , ϕ , ξ , and ζ , where θ is the angle between \vec{v}_∞ and the Earth's heliocentric velocity \vec{V}_\oplus and ϕ is the angle between the plane containing \vec{v}_∞ and \vec{V}_\oplus and the plane containing \vec{V}_\oplus and the ecliptic pole. The deflection angle γ is the angle between \vec{v}_∞ and \vec{v}'_∞ , described by

$$\tan \frac{\gamma}{2} = \frac{c}{b} \quad (33)$$

where $c = GM_\oplus/v_\infty^2$. In addition, simple expressions relate (a, e, i) to (v_∞, θ, ϕ) , and (ω, Ω, ν) to (ξ, ζ, t_0) , where t_0 is the time at which the asteroid passes the node closer to the encounter [14, 15].

A resonance orbit corresponds to certain values of a' and θ' , that can be denoted by a'_0 and θ'_0 . If the post-encounter is constrained in such a way that the ratio of periods between the Earth and the asteroid is k/h , then we have

$$a'_0 = \left(\frac{k^2}{h} \right)^{2/3} \quad (34)$$

$$\cos \theta'_0 = \frac{1 - U^2 - 1/a'_0}{2U} \quad (35)$$

$$= \cos \theta \frac{b^2 - c^2}{b^2 + c^2} + \sin \theta \frac{2c\zeta}{b^2 + c^2} \quad (36)$$

Thus, for a given U , θ , and θ'_0 , we have

$$\cos \theta'_0 = \cos \theta \cos \gamma + \sin \theta \sin \gamma \cos \psi \quad (37)$$

in the pre-keyhole b-plane, which gives the locus of points leading to a given resonant return.

Acknowledgments

This research has been supported in part by the Iowa Space Grant Consortium and a NIAC Phase 2 study. The authors would like to thank William Harding, undergraduate student at Iowa State University, for his technical assistance with some of the improvements to AMiDST. And, a special thank goes to Dr. Paul Chodas for the information and advice he has provided to us on both analytic and numerical keyhole computations.

References

- [1] "General Mission Analysis Tool (GMAT)," <http://gmat.gsfc.nasa.gov/index.html>.
- [2] *LTTT Suite Optimization Tools*, Ed. Timothy A. Reckart, NASA Glenn Research Center Space Science Projects Office, 23 Apr. 2012. <http://microgravity.grc.nasa.gov/SSPO/ISPTProg/LTTT/>.
- [3] Melamed, N., "Development of a handbook and an on-line tool on defending Earth against Potentially Hazardous Objects", *Acta Astronautica* (2012), <http://dx.doi.org/10.1016/j.actaastro.2012.02.021>.
- [4] Vardaxis, G., and Wie, B., "Asteroid Mission Design Software Tool for Planetary Defense Applications," AIAA 12-4872, AIAA/AAS Astrodynamics Specialist Conference, August 2012.

- [5] Vardaxis, G., et al. "Conceptual Design of Planetary Defense Technology Demonstration Mission," AAS 12-128, AAS/AIAA Space Flight Mechanics Meeting, February 2012.
- [6] Vardaxis, G. and Wie, B., "Development of an Asteroid Mission Design Software Tool for Planetary Defense," IAA-PDC13-04-07, 2013 Planetary Defense Conference, Flagstaff, AZ, April 15-19, 2013.
- [7] Pitz, A., et al. "A Hypervelocity Nuclear Interceptor System (HNIS) for Optimal Disruption of Near-Earth Objects," AAIA 12-225, AAS/AIAA Space Flight Mechanics Meeting, February 2012.
- [8] Pitz, A., et al., "Conceptual Design of a Hypervelocity Asteroid Intercept Vehicle (HAIV) and its Flight Validation Mission," GLEX-2012.06.3x12173, 2012 IAF/AIAA Global Space Exploration Conference, Washington D.C., May 22-24, 2012. To appear in *Acta Astronautica*.
- [9] "Near-Earth Object Program." *Near-Earth Object Program*. Ed. Donald K. Yeomans. National Aeronautics and Space Administration. <http://neo.jpl.nasa.gov/index.html>.
- [10] Chodas, P. W. and Yeomans, D., "Orbit Determination and Estimation of Impact Probability for Near Earth Objects." AAS 09-002, AAS/AIAA Space Flight Mechanics Meeting, 2009.
- [11] Pitz, A. et al. "Earth-Impact Probability Computation of Disrupted Asteroid Fragments Using GMAT/STK/CODES," AAS 11-408, AAS/AIAA Astrodynamics Specialist Conference, August 2011.
- [12] Yeomans, D. K., Chodas, P. W., Sitarski, G., Sutowicz, S., and Krolikowska, M., "Cometary Orbit Determination and Nongravitational Forces," Comets II, The Lunar and Planetary Institute, 2004, pp. 137-152.
- [13] Carusi, A., Valsecchi, G. B., and Greenberg, R., "Planetary Close Encounters: Geometry of Approach and Post-Encounter Orbital Parameters," *Celestial Mechanics and Dynamical Astronomy*, Vol. 49, 1990, pp. 111-131.
- [14] Milani, A., Chesley, S. R., Chodas, P. W., and Valsecchi, G. B., "Asteroid Close Approaches: Analysis and Potential Impact Detection," Asteroids III, The Lunar and Planetary Institute, p. 55-69, 2002.
- [15] Valsecchi, G. B., Milani, A., Chodas, P. W., and Chesley, S. R., "Resonant Returns to Close Approaches: Analytic Theory," *Astron. Astrophys.*, 2001.